Venkatram, A. and J. Thé (2003) *Introduction to Gaussian Plume Models*. Chapter 7A of *AIR QUALITY MODELING - Theories, Methodologies, Computational Techniques, and Available Databases and Software. Vol. I - Fundamentals* (P. Zannetti, Editor). Published by The EnviroComp Institute (http://www.envirocomp.org/) and the Air & Waste Management Association (http://www.awma.org/).

Chapter 7A

Introduction to Gaussian Plume Models

Akula Venkatram [(1)] and Jesse Thé [(2)]

[(1)] *College of Engineering, University of California, Riverside, CA 92521-0425, USA*
venky@engr.ucr.edu
[(2)] *Lakes Environmental Software & University of Waterloo – Ontario, Canada*
Jesse@WebLakes.com

Abstract: This section describes the development of models used for regulatory applications at scales of the order of ten kilometers. These models are important because they are used extensively to permit industrial sources and assess risk associated with toxic releases in urban areas. AERMOD and ISC are examples of such models. The foundation of these models is the steady-state plume model that assumes that the concentration distributions normal to the direction of the mean flow are Gaussian.

We first discuss the structure of the Gaussian dispersion model as applied to a point source, and then show how this formulation can be used to estimate impact of other types of sources, such as line and area sources. The realism of models for plume spread determines the usefulness of the Gaussian dispersion model. Plume spread, in turn, depends on atmospheric turbulence. Thus, this section provides a brief description of the atmospheric boundary layer before describing models for plume spread.

We describe different approaches to modeling plume spread of surface and elevated releases in the boundary layer. We then show how the Gaussian dispersion model can be modified to incorporate the effects of buildings and complex terrain on dispersion. The section compares the Gaussian approach to other methods being used to model dispersion. We provide a brief description of one such method, the probability density function method that is currently being used in models of dispersion in the convective boundary layer. The section concludes by emphasizing the usefulness of the Gaussian framework in developing dispersion models for a variety of real world situations.

Keywords: Air pollution, air quality, air pollution model, AERMOD, ISC, dispersion, building effects. Gaussian dispersion model, regulatory model, atmospheric boundary layer, complex terrain dispersion, convective boundary layer, stable boundary layer.

1 Introduction

Air pollution models play an important role in the implementation of air pollution regulations. For example, before an industrial plant can be constructed, its impact on air quality is determined through an air pollution model to show that emissions from the plant do not lead to ambient concentrations that are above a regulated level. In the United States, the Industrial Source Complex (ISC) model is used to make such permitting decisions. U.S. regulations that govern air toxics recommend the use of the ISC model to quantify risk associated with emissions of toxic chemicals in urban areas. Air pollution models that include chemistry are used to make decisions to control emissions that are precursors of ozone and acidifying pollutants. Such decisions can have multimillion-dollar implications associated with installing equipment to reduce emissions, or delaying or even disallowing the construction of the industry responsible for the emissions.

This chapter examines air pollution models applicable to scales of the order of tens of kilometers. The effects of chemistry are assumed to be negligible at these scales, although this might not be always true. These models assume are commonly referred to as Gaussian models because they assume that the concentration distributions in the vertical and the horizontal are described by the Gaussian function.

The chapter also provides the background necessary to understand the approach used in the formulation of such models. This includes the essentials of the micrometeorology used to construct the inputs for the model.

2 The Point Source in the Atmospheric Boundary Layer

Most short-range dispersion models are based on the assumption that meteorological conditions are spatially homogeneous and vary little with time during the period of interest, which is typically one hour. This is equivalent to saying that the time scale governing the variation in meteorology is greater than the time of travel between source and receptor. If the meteorological time scale is one hour, and the wind speed is 5 m/s, the assumption of steady state is not likely to be valid for distances much greater than 10 km. At lower wind speeds, the "valid" distances become smaller. In spite of these limitations, steady state plume models are often applied beyond their range of applicability with the justification that the concentration at the receptor is representative of that when the plume eventually reaches the receptor. In principle, dispersion during unsteady and spatially varying conditions can be treated with puff or particle models, which attempt to model the dispersion of puffs or particles as the unsteady wind field carries them along their trajectories. This paper will not discuss models based on puff dispersion.

Models such as ISC and AERMOD are based on the steady state Gaussian dispersion equation. If the release point is taken to be the origin (**z**=0), with the **x**-axis of the co-ordinate system aligned along the wind direction at the source, the time averaged (typically one hour) concentration field can be described in terms of the Gaussian distribution (See Figure 1):

$$C(x,y,z) = \frac{Q}{2\pi\sigma_y\sigma_z U}\exp\left[-\frac{z^2}{2\sigma_z^2}-\frac{y^2}{2\sigma_y^2}\right], \qquad (1)$$

where **y** is the cross-wind co-ordinate, **Q** is the source strength (mass/time), **U** is the time-averaged wind speed at source height, and σ_y and σ_z are the plume spreads normal to the mean wind direction. Equation (1) can be "derived" from the mass conservation equation after making assumptions about turbulent transport. Because these assumptions cannot be readily justified, it is just as valid to simply postulate Equation (1) as an empirical description of observations.

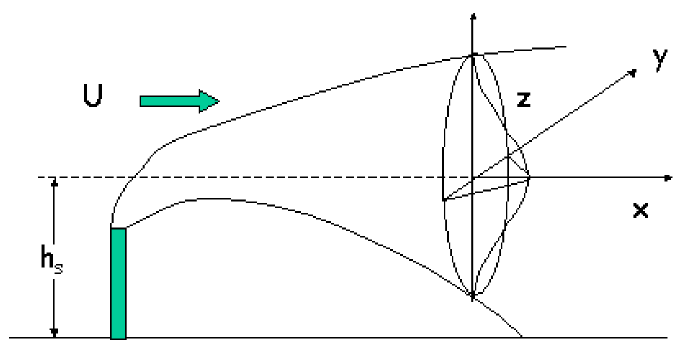

Figure 1. Gaussian distribution used to model plume from point source. For the time being, we have ignored the effects of the impermeable ground on the concentration field. Equation (1) assumes that along-wind dispersion is much smaller than transport by the mean wind. This assumption breaks down when the mean wind is comparable to the turbulent velocity along the wind, σ_u. The form of the dispersion model under such low wind speed conditions is discussed in a later section.

The effect of the ground on concentrations is accounted for by making sure that there is no flux of material through the ground, which we now take to be **z**=0. The mathematical trick to achieve this is to place an "image" source at a distance $z = -h_s$, where h_s is the height of the source above ground. The upward flux from this image source essentially cancels out the downward flux from the real source without affecting the mass balance. Then, the concentration becomes

$$C(x,y,z)=\frac{Q}{2\pi\sigma_y\sigma_z U}\exp\left[-\frac{y^2}{2\sigma_y^2}\right]\left\{\exp\left[-\frac{(z-h_s)^2}{2\sigma_z^2}\right]+\exp\left[-\frac{(z+h_s)^2}{2\sigma_z^2}\right]\right\} \quad (2)$$

In the real atmosphere, dispersion in the upward direction is limited by the height of the atmospheric boundary layer. This limitation of vertical mixing is incorporated into the Gaussian formulation by "reflecting" material off the top of the mixed layer. Then, Equation (2) can be modified to account for the infinite set of "reflections" from the ground and the top of the mixed layer. When the pollutant is well mixed through the depth of the boundary layer, $\mathbf{z_i}$, the expression for the concentration becomes:

$$C(x,y)=\frac{Q}{\sqrt{2\pi}\sigma_y z_i}\exp\left(-\frac{y^2}{2\sigma_y^2}\right) \quad (3)$$

The Gaussian formulation for a point source can be used to model both volume as well as point sources because each of these source types can be discretized into point sources; the associated concentrations are simply the sums of the contributions from these point sources.

In applying Equation (2) to model line or volume sources, it is important to make sure that the x co-ordinate system is aligned along the mean wind direction. Specifically, if (X_r,Y_r) and (X_s,Y_s) are the co-ordinates of the receptor and the source in an arbitrary co-ordinate system, and θ is the angle that the mean wind velocity vector makes with x-axis, then the co-ordinates used in the Gaussian equation are given by (See Figure 2)

$$\begin{aligned} x &= X\cos\theta + Y\sin\theta \\ y &= X\sin\theta - Y\cos\theta \end{aligned} \quad (4)$$

where

$$\begin{aligned} X &= X_r - X_s \\ Y &= Y_r - Y_s \end{aligned} \quad (5)$$

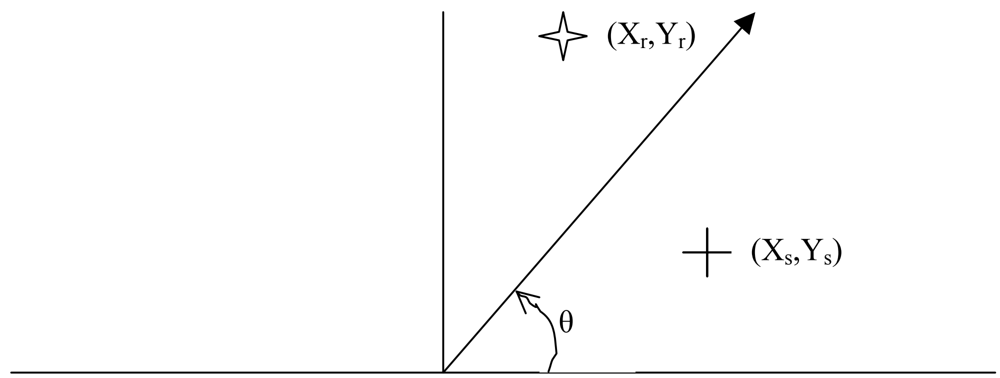

Figure 2. Co-ordinate system to derive Equations (4) and (5). θ is the angle that the mean wind velocity vector makes with x-axis.

Consider modeling dispersion from a ground-level line source such as freeway. If we align the line source along the Y axis, and the emission rate per unit length of the line source is **q**, the expression for the concentration associated with an elemental length $\mathbf{dY_s}$ becomes

$$dC(X_r, Y_r) = \frac{qdY_s}{\pi U \sigma_y \sigma_z} \exp\left(-\frac{y^2}{2\sigma_y^2}\right) \exp\left(-\frac{z^2}{2\sigma_z^2}\right), \tag{6}$$

where the lower case symbols refer to the co-ordinate system with the x-axis along the mean wind.

Then, the concentration associated with a line-source between Y_1 and Y_2 becomes

$$C(X_r, Y_r) = \int_{Y_1}^{Y_2} \frac{qdY_s}{\pi U \sigma_y \sigma_z} \exp\left(-\frac{y^2}{2\sigma_y^2}\right) \exp\left(-\frac{z^2}{2\sigma_z^2}\right) \tag{7}$$

The expression assumes a simple form if the mean wind is perpendicular to the road ($\theta=0^o$) and the line source is infinitely long (this is a good approximation if a receptor is close to the line source)

$$C(X_r, Y_r) = \sqrt{\frac{2}{\pi}} \frac{q}{U\sigma_z} \exp\left(-\frac{z^2}{2\sigma_z^2}\right) \tag{8}$$

where the plume spread, $\boldsymbol{\sigma_z}$, is evaluated at $\mathbf{x=X_r}$. If the wind blows at a "small" angle, $\boldsymbol{\theta}$, to the **X** axis, we can still use Equation (8) by replacing **U** by $\mathbf{U\cos\theta}$, and evaluating vertical plume spread at $\mathbf{X_r/\cos\theta}$. But this only an approximation that breaks down when **θ** exceeds the smaller of the angles formed by joining the ends of the line source to the receptor in question.

Models for the plume spread parameters, σ_y, and σ_z determine the usefulness of the concentration estimates from the Gaussian model. Most of the currently used regulatory dispersion models, such as ISC, use expressions derived empirically from field experiments. The new generation of regulatory dispersion models, such as AERMOD (Cimorelli et al., 2002), estimate dispersion using information, measured or modeled, on the mean and turbulent structure of the atmospheric boundary layer. The next section on the atmospheric boundary provides the background necessary to understand the formulation of these dispersion curves, described in section 4.

3 The Atmospheric Boundary Layer

Turbulence in the atmospheric boundary layer is generated by wind shear and buoyancy associated with radiative heating at the ground. During the daytime, sensible heating at the surface results in parcels of air that are warmer, and hence less dense than their surroundings. These parcels are subject to buoyancy forces that accelerate them upwards. The mixing induced by these moving parcels gives rise to the boundary layer or mixed layer, whose growth is inhibited by a layer in which the rising parcels are denser than their surroundings. This layer, referred to as an inversion, is characterized by increasing temperature with height. This inversion usually develops when there is large-scale downward motion or subsidence of the air. It can be shown that at heights below about a tenth of the mixed layer height, z_i, buoyancy generates turbulent velocities given by:

$$\sigma_w = 1.3 u_f ;\ z \le 0.1 z_i \tag{9}$$

where the free convection velocity scale, $\mathbf{u_f}$ is defined by:

$$u_f = \left(\frac{g}{T_s} Q_o z \right)^{1/3} \tag{10}$$

In Equation (9), $\mathbf{Q_o}$ is the surface kinematic heat flux, which is the sensible heat flux (Watts/m^2) divided by the product of the density and the specific heat of air, and $\mathbf{T_s}$ is the surface temperature in degrees Kelvin. The heat flux, $\mathbf{Q_o}$, is taken to be positive when it is directed away from ground and into the atmosphere as during the daytime, and is negative when it is into the ground as during most nights.

Between $\mathbf{0.1z_i}$ and close to the top of the mixed layer, $\boldsymbol{\sigma_w}$ associated with buoyancy production of turbulence is proportional to the convective velocity scale given by

$$w_* = \left(\frac{g}{T_s} Q_o z_i\right)^{1/3} \tag{11}$$

where $\mathbf{z_i}$ is the mixed layer height. In this region, we find that

$$\sigma_w = \sigma_v = \sigma_u \cong 0.6 w_* \tag{12}$$

It is found that $\boldsymbol{\sigma_u}$ and $\boldsymbol{\sigma_v}$ are also proportional to $\mathbf{w_*}$, even below $\mathbf{0.1z_i}$.

Where turbulence production is dominated by wind shear, $\boldsymbol{\sigma_w}$ close to the ground is roughly proportional to the surface friction velocity, $\mathbf{u_*}$

$$\sigma_w = 1.3 u_* \tag{13}$$

where u_* is related to the shear stress at the ground, τ_o, through

$$u_* = \sqrt{\frac{\tau_o}{\rho_a}} \tag{14}$$

where $\boldsymbol{\rho_a}$ is the density of air. The absolute value of the Monin-Obukhov length, **L**, is roughly the height at which the turbulent velocity generated by buoyancy is equal to that produced by shear,

$$L = -\frac{T_s u_*^3}{gkQ_o} \tag{15}$$

where the Von Karman constant **k**=0.4.

Thus, shear production of turbulence dominates that by buoyancy at heights below the Monin-Obukhov length. **L** is usually negative during the daytime when the heat flux is into the atmospheric boundary layer, and positive during nighttime when the heat flux is directed towards the ground.

In describing the structure of the atmospheric boundary layer, it is convenient to define a potential temperature at given height with temperature **T**, and pressure, **p**,

$$\theta = T\left(\frac{p_0}{p}\right)^{\frac{R_a}{C_p}} \tag{16}$$

where $\mathbf{p_0}$=1000 mb is a reference pressure, $\mathbf{R_a}$ is the gas constant, and $\mathbf{C_p}$ is the specific heat of air. The potential temperature, **θ,** represents the temperature that a parcel with temperature, **T**, would acquire if it is moved adiabatically from **p** to $\mathbf{p_0}$.

The potential temperature definition allows us to make statements about the stability of a parcel of air when it is displaced adiabatically without worrying about the effects of pressure changes in the atmosphere. It can be shown that a parcel resists vertical motion in an atmosphere in which the potential temperature increases with height; it is in stable equilibrium. A decreasing potential temperature denotes an unstable atmosphere, while a potential temperature that is constant with height characterizes an atmosphere that is neutral to parcel motion.

In the daytime boundary layer, the potential temperature decreases with height near the surface. Above a tenth of the mixed layer height, the potential temperature and the horizontal velocity are relatively uniform because of vigorous vertical mixing. The mixed layer is usually capped by a sharp temperature inversion, and the velocity can also change rapidly across the inversion.

When the sun sets, turbulence energy production by buoyancy ceases. Over a period of an hour, the turbulence in the mixed layer collapses, and shear becomes the primary mechanism for the production of turbulence. Because the ground is initially warmer than the atmosphere, the thermal radiation leaving the ground exceeds that being supplied by the atmosphere. This deficit leads to a cooling of the ground.

Initially, both the sensible heat flux and the ground heat flux are directed away from the earth's surface. The surface cools rapidly, and a point is reached at which the ground becomes colder than the layers above in the atmosphere. At this stage, the heat flux from the atmosphere is directed towards the earth's surface, and the surface boundary layer becomes stable with the potential temperature increasing with height.

The stable potential temperature gradient in the nighttime boundary layer suppresses the production of turbulence because it opposes vertical motion. Under these circumstances, shear production of turbulence is matched by the destruction associated with the stable temperature gradient and viscous dissipation. This balance between these processes of production and destruction leads to relatively small levels of turbulence in the nocturnal boundary layer. We know that turbulence levels in the stable boundary layer are of the order of the surface friction velocity. However, estimating the height of the stable boundary layer or the variation of turbulence levels with height is an uncertain exercise. The horizontal turbulent velocities in the stable boundary layer do not appear to be related to micrometeorological variables. They are affected by mesoscale flows and local topography, which are difficult to characterize using models.

The next section describes how regulatory models use information on the turbulent and mean flow fields in the atmospheric boundary layer to estimate plume spreads.

4 Dispersion in the Atmospheric Boundary Layer

ISC uses plume spread formulations based on those derived empirically by Pasquill (1961) in the 1960s from observations made during the Prairie Grass dispersion experiment conducted in Nebraska in 1956 (Barad, 1958). These formulations were modified subsequently by Gifford and Turner, and are commonly referred to as the Pasquill-Gifford-Turner (PGT) curves. For dispersion in urban areas, ISC uses the McElroy-Pooler curves that are derived from experiments conducted in St. Louis, Missouri (McElroy and Pooler, 1968).

The dispersion curves are keyed to stability classes that are related to ranges in the wind speed and incoming solar radiation. The wind speed, measured at 10 m, is an indicator of turbulence produced by shear, while the incoming solar radiation is a surrogate for the sensible heat flux, which generates turbulence. Thus, the stability classes contain information on shear and buoyancy produced turbulence.

Classes A, B, and C correspond to unstable conditions when buoyancy production of turbulence adds to that due to shear. The sensible heat flux under these conditions is upward. Class A, the most unstable, is associated with the most rapid dispersion rates; the plume sigmas for a given distance decrease as we go from class A to C. Class D corresponds to neutral conditions when turbulence production is dominated by shear. Classes E and F are associated with stable conditions. Class F corresponds to the lowest dispersion rates. The dispersion curves are only functions of distance from the source, and can be cast into the form

$$\sigma_z = ax^b \tag{17}$$

where the coefficients "**a**" and "**b**" generally increase as the stability classes range from E to A. Thus, 6 dispersion curves are used to describe the entire range of possible dispersion conditions.

The major advantage of the PGT curves is that they are based on observations, and thus provide realistic concentration estimates under a variety of meteorological conditions. Their shortcoming is that they are derived from dispersion of surface releases, and are thus not applicable to elevated releases. Furthermore, their formulation does not allow the use of on-site turbulence levels to describe dispersion more accurately than the "broad brush" PGT curves.

In the more recently formulated models (Weil, 1985), such as AERMOD, the expressions for plume spread are based on theoretical analysis first proposed by Taylor (1921). His equation describes the variance of particle positions as a function of travel time from a fixed point of release in a flow that is steady and the turbulence statistics do not depend on location. Rather than present all of his analysis, we will highlight the major results using the asymptotic behavior of the plume spread (Csanady, 1973),

$$\begin{aligned} \sigma_y &= \sigma_v \tau \quad \text{for } \tau << T_{Lv} \\ \sigma_y &= \sigma_v \left(2\tau T_{Lv}\right)^{1/2} \quad \text{for } \tau >> T_{Lv} \end{aligned} \tag{18}$$

where τ is the travel time from the source, given by

$$\tau = \frac{x}{U} \tag{19}$$

and $\boldsymbol{\sigma_v}$ is the standard deviation of the horizontal turbulent velocity fluctuations. A similar expression applies to the vertical spread of the plume.

In Equation (18), $\mathbf{T_{Lv}}$ is the Lagrangian time scale, which can be formally defined in terms of the statistics of the turbulent flow. For our purposes, it is sufficient to interpret the time scale as roughly the time over which a particle retains its initial velocity. For small travel times, a particle's velocity remains essentially unchanged from its value at the release point, and the particle trajectory is a straight line. This explains the result that, for small travel times, the spread of particles is proportional to the travel time from the source (Equation (18)). On the other hand, when the travel time is large compared to the Lagrangian time scale, the plume spread is proportional to the product of the "average" step size, $\sigma_v T_{Lv}$, and the square root of the number of steps, τ / T_{Lv}, taken by the particle.

The new generation of dispersion models, such as AERMOD, relates dispersion to atmospheric turbulence using the theoretical framework described earlier. The problem in doing so is that the theory applies to a boundary layer in which the mean and turbulent properties are constant in space and time. To apply it to a real boundary layer in which the properties are highly inhomogeneous, we can use one of two approaches. The first is to average the turbulence and mean properties over the region of interest, and use the average properties in the (homogeneous) formulations discussed earlier. This is not as straightforward as it seems because the limits of the average requires an estimate of the plume dimensions, which in turn depends on the average properties. Furthermore, the averaging procedure is necessarily arbitrary. The validity of the method needs to be established by comparing the results obtained from the formulations with observations or theory that accounts for inhomogeneity more explicitly. In general, empirical knowledge derived from observations plays a major role in the development of practical models of dispersion. As in most turbulence research, theory can suggest plausible forms for a dispersion model, but the model almost always contains parameters that have to be estimated from observations.

Even if we could treat the boundary layer as vertically homogeneous, the presence of boundaries, such as the ground and the top of the mixed layer, makes it difficult to estimate the Lagrangian time scale, T_{Lv}, from a priori considerations. Thus, the time-scale is often treated as an empirical parameter that is derived by fitting plume spread expressions to observations. Let us illustrate this by using an expression that is often used to describe plume spread

$$\sigma_y = \frac{\sigma_v \tau}{\left(1 + \tau / 2T_{Lv}\right)^{1/2}} \tag{20}$$

Note that Equation (20) satisfies the asymptotic limits given by Equation (18). We then postulate an expression for T_{Lv} in terms of a length scale **l** as follows

$$T_{Lv} = \frac{l}{\sigma_v} \tag{21}$$

The length scale is taken to be proportional to a length characterizing the eddies responsible for transport, and the constant of proportionality is obtained by fitting estimates of plume spread from Equation (20) to observations. In AERMOD, the vertical spread for elevated releases in the stable boundary layer is given by an expression similar to Equation (20).

The second approach to accounting for inhomogeneity in the boundary layer is based on the solution of the species conservation equation

$$\frac{\partial C}{\partial t} + \frac{\partial}{\partial x_i}\left(U_i C\right) = \frac{\partial}{\partial x_i}\left(K^i \frac{\partial C}{\partial x_i}\right) \tag{22}$$

where $\mathbf{K^i}$ is the so-called eddy diffusivity, and the superscript negates the summation convention. The eddy diffusivity is defined as the ratio of the turbulent mass flux to the local mean concentration gradient. The concept, which is based on an analogy with molecular transport, cannot be justified rigorously for turbulent transport. However, it has heuristic value, and is useful for developing semi-empirical models of turbulent transport.

It can be shown that the eddy diffusivity concept is most applicable when the scale of concentration variation, the plume spread, is larger than the scale of the eddies responsible for plume spreading. In the surface boundary layer, plume spread in the vertical direction is comparable to the length scale of the eddies responsible for vertical transport. It turns out that that the eddy diffusivity concept is useful in the surface boundary layer, where semi-empirical theories, referred to as Monin-Obukhov similarity, provide useful relationships between velocity and temperature gradients and the corresponding heat and momentum fluxes. These relationships can be used to derive eddy diffusivities for heat and momentum, which can be used to describe dispersion by evaluating them at some fraction of the plume height.

Existing regulatory models for short-range dispersion do not use the eddy diffusivity based mass conservation equation to avoid the associated numerical effort and to make the most efficient use of observations of plume spread. However, the eddy diffusivity concept can be useful in deriving expressions for plume spread in the inhomogeneous surface layer. For example, AERMOD's expressions for plume spread are based on this approach (Venkatram, 1992):

$$\begin{aligned}\sigma_z &= \sqrt{\frac{2}{\pi}}\frac{u_* L}{U}\bar{x}\,;\text{for } \bar{x} \le 1.4 \\ &= \sqrt{\frac{2}{\pi}}\frac{u_* L}{U}1.12\bar{x}^{2/3}\,;\text{for } \bar{x} > 1.4,\ L > 0 \\ &= \sqrt{\frac{2}{\pi}}\frac{u_* |L|}{U}\frac{\bar{x}}{(1+0.006\bar{x}^2)^{-1/2}}\,;\text{for } L < 0\end{aligned} \tag{23}$$

where $\bar{x} = x/|L|$, and the wind speed **U** corresponds to an average over the surface layer. In practice, the ground-level concentration is insensitive to the choice of **U**, because the dilution is determined by the combination $\boldsymbol{\sigma_z U}$. These expressions provide a good description of the cross-wind integrated concentrations observed during the Prairie Grass experiment (see Van Ulden, 1978 for a listing of the data).

In AERMOD, the horizontal spread, $\boldsymbol{\sigma_y}$, is based on an equation similar to Equation (20). The Lagrangian time scale was derived by fitting the equation to observations of plume spread from the Prairie Grass experiment.

In order to use the Gaussian dispersion model, we need estimates of plume rise, which is treated in Chapter 9. Dispersion and plume rise are also affected by the presence of buildings in the vicinity of the source. This is treated in the next section.

5 Building Downwash

Buildings and other structures near a relatively short stack can have a substantial effect on plume transport and dispersion, and on the resulting ground-level concentrations that are observed. The "rule of thumb" is that a stack should be at least 2.5 times the height of adjacent buildings to avoid the effects of the buildings. Much of what is known of the effects of buildings on plume transport and diffusion has been obtained from wind tunnel studies and field studies.

When the airflow meets a building (or other obstruction), it is forced up and over the building. On the lee side of the building, the flow separates, leaving a closed circulation containing lower wind speeds (see Figure 3). Farther downwind, the air flows downward again. In addition, there is more shear and, as a result, more turbulence. This is the turbulent wake zone.

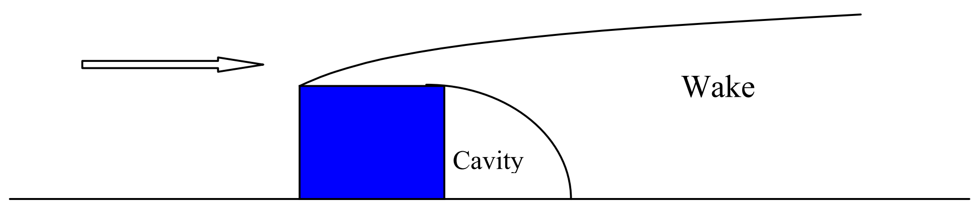

Figure 3. Formation of cavity and wake behind building.

If a plume gets caught in the cavity, concentrations next to the building can be relatively high. If the plume escapes the cavity, but remains in the turbulent wake, it may be carried downward and dispersed more rapidly by the turbulence. This can result in either higher or lower concentrations than would occur without the building, depending on whether the reduced height or increased turbulent diffusion has the greater effect. The height to which the turbulent wake has a significant effect on the plume is generally considered to be about the building height plus 1.5 times the lesser of the building height or width. This results in a height of 2.5 building heights for cubic or squat buildings, and less for tall, slender buildings. Since it is considered good engineering practice to build stacks taller than adjacent buildings by this amount, this height is called the "good engineering practice" (GEP) stack height.

Most treatments of building effects on dispersion are based on incorporating two effects: 1) the effective reduction of source height associated with the trapping of pollutants in the cavity, and 2) the increased turbulence in the building wake. If the emissions are entrained into the cavity, the source is assumed to be at ground-level, but the plume is assigned initial values to account for the fact that the emissions originate from a cavity whose size scales with the dimensions of the building. For example, the initial spreads of the plume can be taken to be

$$\sigma_{yo} = \alpha w$$
$$\sigma_{zo} = \beta h \tag{24}$$

where **w** and **h** are the width and height of the building, and **α** and **β** are constants. Alternatively, these initial spreads can be modeled in terms of a "virtual" source at ground-level at an upwind distance that results in these spreads. For example, the upwind distance of the location of the virtual source resulting in the initial horizontal spread can be calculated from

$$\sigma_{yo} = a x_o^b \tag{25}$$

where the coefficients, **a** and **b**, correspond to atmospheric stability of the incoming flow. This virtual distance $\mathbf{x_o}$ is added to the source-receptor distance used to estimate horizontal spread.

The fraction of the emissions that is entrained into the building cavity is taken to be a function of the stack height, and the building height. The fraction that is not entrained into the cavity is treated as a conventional point source, except that plume dispersion is enhanced to account for the increased turbulence levels in the building cavity. The concentration at a downwind receptor is then a sum of the concentrations from the elevated source and the ground-level source, corresponding to the emissions from the cavity. Current models use approaches based on these ideas.

In the original version of the U.S. EPA ISC (Industrial Source Complex) Model (Bowers, et al., 1979), building downwash calculations were included for any stack within five times the lesser of the height or the width (the so-called "5L" rule) of building and less than GEP based on the same building (Huber and Snyder, 1982). Calculations were made assuming the stack was located at the highest point of the deflected flow, essentially at the lee edge of the building, and using the maximum projected width (of all wind directions). This was essentially the worst-case location of the stack, regardless of where the stack really was located in relation to the building, and the worst-case wind direction, regardless of the actual wind direction. In addition, the full effect of the building wake on plume dispersion was used, even when the plume had risen above the top of the wake region.

The ISC model was modified around 1986 to incorporate an approach developed by Schulman and Scire (1980). As implemented in the model, the Schulman-Scire downwash algorithm was used for stack heights less than 1.5 building heights, while the older Huber-Snyder approach was retained for the higher stack. The most apparent change implemented by this approach is that the amount of building downwash would change with wind direction, thus allowing for the effects of the change in building profile with different wind directions. The Schulman-Scire downwash algorithm also accounts for reduced plume rise due to initial plume dilution that results from building downwash. Thirdly, this algorithm calculates a reduced effect of downwash on a plume that has risen higher, and is exposed to less downwash-induced turbulence.

As implemented in the ISCST3 modeling system, a determination is made as to whether building downwash due to a particular building affects the plume from a stack based on wind direction. This is calculated on an objective basis by a preprocessor program called BPIP (Building Profile Input Program), which is a part of the ISCST3 system. When more than one building, or more than one tier on a building, may affect the plume, BPIP also calculates which building or tier dominates, and provides the ISCST3 model with building height and projected width for the appropriate building or tier for each wind direction. More details on the treatment of building wake effects in ISCST3 can be found in U.S. EPA (1995a) and U.S. EPA (1995b).

The inclusion of the PRIME algorithm (Schulman, et al., 2000) to compute building downwash has produced more accurate results in air dispersion models. Unlike the earlier algorithms used in ISC3, the PRIME accounts for a) the location of the stack relative to the building, b) the deflection of streamlines up over the building and down the other side, c) the effects of the wind profile at the plume location for calculating plume rise, d) pollutants captured in the recirculation cavity to be transported to the far wake downwind (this is ignored in the earlier algorithms), and e) discontinuities in the treatment of different stack heights, which were a problem in the earlier algorithms. Details of the PRIME algorithm are given in Schulman, et al. (2000).

6 Terrain Treatment

Several complicated processes govern dispersion in complex terrain. Under unstable conditions, the plume is depressed towards the surface of the obstacle as it goes over it. The implied compression of the streamlines is associated with a speed-up of the flow and an amplification of vertical turbulence. Under stable conditions, part of the flow flowing towards an obstacle tends to remain horizontal, while the other part climbs over the hill. Experiments show (Snyder *et al.*, 1983) that this tendency for the flow to remain horizontal can be described using the concept of the dividing streamline height, denoted by H_c. Below this height, the fluid does not have enough kinetic energy to surmount the top of the hill; a plume embedded in the flow below H_c either impacts on the hill or goes around it. On the other hand, the flow and hence the plume above H_c can climb over the hill. Terrain features can rise toward the plume, deflecting its flow over or around, or allowing the plume to come in contact with the terrain. In convective (unstable) conditions, the airflow, and thus the plume, will be forced over the terrain obstacle. On the lee side of the obstacle, a wake or cavity may occur in the flow, resulting in high concentrations on that side of the terrain feature.

The alignment of ridges and valleys can channel the flow. This can result in high concentrations appearing in areas quite different than would be expected if this effect were not accounted for. The presence of hills and valleys can also help to create local wind flows. These flows may alter the transport of low-level plumes. Modeling these flows using wind data from above or distant from the site may result in incorrect modeling results. Conversely, wind measurements that are influenced by these local flows, if used to model a tall stack source that emits above the local flow, can also result in incorrect modeling results. One example is the case of a narrow valley with a north to south orientation. In the morning, the sun will first heat the west wall of the valley. This warmer air will rise, creating a cross-valley flow from east to west (in the absence of strong winds aloft). Conversely, in the evening, the east wall will be heated more, resulting in a cross-valley flow from the west.

Accounting for these effects in air quality models presents a significant challenge. The effects cannot be ignored in regulatory modeling, since terrain effects generally contribute to higher concentrations than would be observed in flat terrain situations. On the other hand, representing terrain effects accurately may require the use of computational fluid dynamics models, or other modeling approaches that require extensive computer resources, and are difficult and time-consuming to use.

6.1 Approaches Taken in Short-Range Models

Early attempts to incorporate terrain heights into regulatory air quality models were to simply subtract the terrain elevation above the source from the calculated plume height, an approach used in the ISCST2 model (USEPA, 1992). Since, in reality, the plume will be deflected along with the wind, this modeling approach often results in severe over predictions of concentrations. In response to this problem, some fairly simple complex terrain screening models were developed, including the use of a “half-height correction,” and modified plume impact.

The “half-height” correction assumed that the plume height in terrain (usually under stable conditions, i.e., P-G stabilities E and F, although some models use it for neutral and unstable cases as well) would rise at half the rate as the terrain would rise between the source and receptor. While the theoretical basis for this approach is weak, it prevents the direct impact of plume centerline on the terrain feature, giving concentration estimates that are, at least, appear to be more reasonable.

The COMPLEX-I model (U.S. EPA, 1995) uses this same formulation for P-G stabilities E and F, at any wind speed, and a half-height terrain adjustment for P-G stabilities A through D. For regulatory applications, the EPA initially allowed the use of COMPLEX-I in combination with ISCST2. For each hour and source-receptor combination, when the terrain was below *stack* height, called "simple terrain," ISCST2 would be used; when the terrain was above *plume* height, called "complex terrain," COMPLEX-I would be used; and between the two, called "intermediate terrain," both would be used and the larger of the two calculated concentrations selected. This was a complicated approach, which was best implemented in a computer code.

The Complex Terrain Dispersion Model (CTDMPLUS, Perry, 1992) accounts for the major effects associated with the concept of the dividing streamline height described in the previous section. AERMOD incorporates a semi-empirical model (Venkatram *et al.*, 2001) that mimics the major features of CTDM. It assumes that the concentration at a receptor, located at a position (x, y, z), is a weighted combination of two concentration estimates: one assumes that the plume is horizontal, and the other assumes that the plume climbs over the hill.

The concentration associated with the horizontal plume dominates during stable conditions, while that caused by the terrain-following plume is more important during unstable conditions. These assumptions allow us to write the concentration, $C(x, y, z)$, as

$$C(x, y, z) = fC_f(x, y, z) + (1 - f)C_f(x, y, z_e) \quad (26)$$

The first term on the right-hand side of Equation (26) represents the contribution of the horizontal plume, while the second term is the contribution of the terrain-following plume. The concentration, $C_f(x, y, z)$, is that associated with a plume unaffected by the terrain; the plume axis remains horizontal. In the first term, $C_f(x, y, z)$ is evaluated at the receptor height, $\mathbf{z}$, to simulate a horizontal plume. In the second term, the concentration is evaluated at the height of the receptor above local terrain, $\mathbf{z_e}$, to simulate the plume following the terrain contour.

The weighting factor, $\mathbf{f}$, is a function of the fraction of the plume above the dividing streamline height. When the entire plume lies below $\mathbf{H_c}$, $\mathbf{f}$ goes to unity, and the concentration corresponds to a plume that does not see the hill. When the dividing streamline height goes to zero under unstable conditions, $\mathbf{f}$ becomes ½. This means, that under unstable conditions, the concentration at an elevated receptor is the average of the contributions from the horizontal plume and the terrain-following plume.

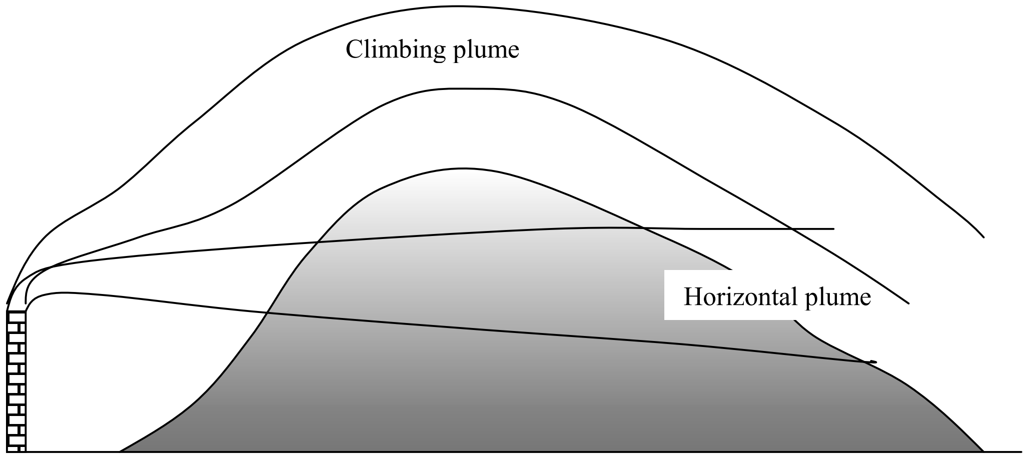

Figure 4. The two states of the plumes used to formulate the complex terrain model.

This formulation of the complex terrain model ensures that the model estimates are sensible in that they range between values corresponding to two limits of plume behavior. This simple semi-empirical model has been tested at several complex terrain sites, and it performs at least as well as CTDM in the limited task of describing concentration statistics.

7 Modifications to the Gaussian Framework

New models, such as AERMOD, incorporate physics that cannot be readily accommodated within the framework of the Gaussian distribution of the concentration. One example is dispersion in the unstable boundary layer. In the unstable boundary layer, both the mean wind and turbulence levels are relatively uniform above a height of about $1/10^{th}$ of the boundary layer height. In principle, this should allow a straightforward application of Taylor's equations for plume spread in the Gaussian expression. However, the Gaussian equation is not appropriate because the turbulent vertical velocities in the middle of the convective boundary layer do not follow a Gaussian distribution; the distribution has a negative mode, and has a long positive tail as shown in Figure 5. This implies that material released in the middle of the boundary layer has a greater probability of being caught in downdrafts than in updrafts. This leads to the descent of the plume centerline, which cannot be described with a symmetric Gaussian model. Several approaches have been used to capture this feature of dispersion of elevated releases in the convective boundary layer.

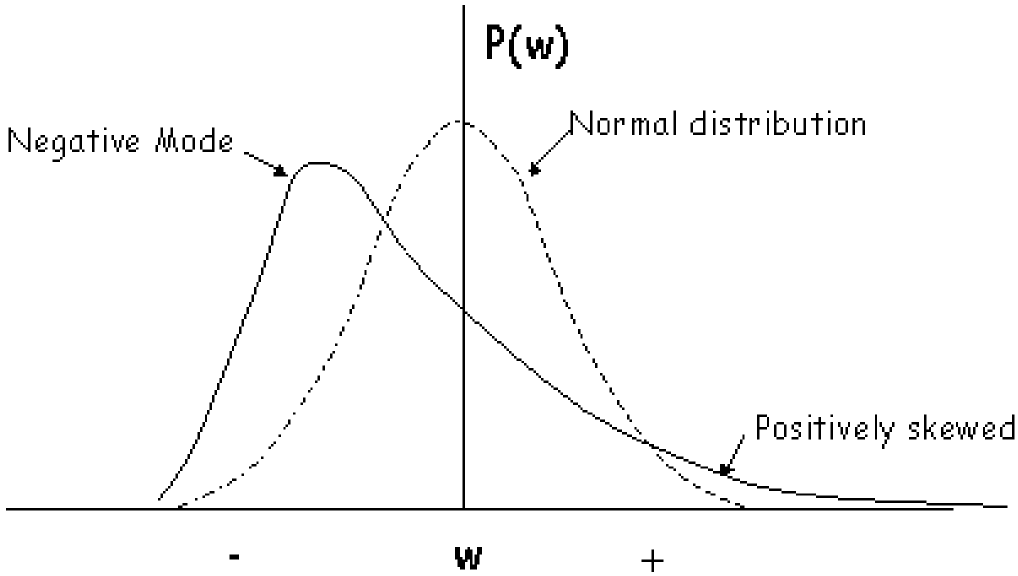

Figure 5. Vertical Velocity Distribution in the CBL.

AERMOD uses what is commonly referred to as the probability density function (pdf) approach, which assumes that a particle does not forget its velocity at release. This implies that the crosswind-integrated concentration at ground-level is determined by the probability density function of vertical velocities at the source.

$$\overline{C}^y = \frac{2Q}{U\sigma_z}\sigma_w P\left(w = -\frac{uh}{x}\right) \tag{27}$$

where **P(w=-uh/x)** is the probability density function evaluated at the vertical velocity that brings plume material from the elevated release to the receptor at **x** in a straight line. The factor 2 accounts for reflection at the ground.

It is easy to see that the Gaussian formulation is recovered if the pdf is Gaussian. AERMOD uses a skewed pdf that allows for the plume centerline to descend towards the ground, and leads to concentrations that can be over 30% higher than that associated with a Gaussain pdf (See Venkatram, 1993). The actual formulation in AERMOD combines plume rise with dispersion, and mimics the non-Gaussian pdf in Equation (27) as a sum of two Gaussian distributions, which results in the required mode and skewness.

7.1 Other Features in Regulatory Models

Regulatory models also need to account for special features of urban areas. In ISC, dispersion in urban areas is treated using empirical dispersion curves derived from tracer experiments conducted in St. Louis (McElroy and Pooler, 1968).

These so-called McElroy Pooler curves, which are keyed to stability classes, lead to enhanced dispersion in urban areas.

AERMOD treats urban dispersion by accounting for the processes that lead to the enhancement of turbulence in urban areas. When rural air flows into a warmer urban area, the boundary layer becomes convective because of surface heating. Thus, when the rural boundary layer is stable during the night, the urban boundary layer can be convective. AERMOD accounts for this effect by formulating an upward heat flux and a boundary layer height in terms of the urban-rural temperature difference, which in turn is parameterized in terms of the population of the urban area. Then, a convective velocity scale is calculated using this heat flux, and the associated boundary layer height. This convective velocity scale is then used to calculate a turbulence profile, which is then added to that from the rural area. The increased roughness over an urban area is included in the calculation of the rural turbulence profile.

When the wind speeds become comparable to the turbulent velocities, it becomes necessary to account for dispersion along the wind direction, which is neglected in most regulatory dispersion models, including ISC. Such conditions are common in urban areas, where buildings can enhance turbulence and reduce the mean flow. Neglecting along-wind dispersion can lead underestimation of concentrations upwind of the source.

AERMOD accounts for low wind speed conditions by assuming that the concentration is a weighted average of concentrations in two possible states: a random spread state, and plume state. In the random spread state, the release is allowed to spread equally in all directions. Then, the weighted horizontal distribution is written as:

$$H(x,y) = f_r \frac{1}{2\pi r} + (1-f_r)\frac{1}{\sqrt{2\pi}\sigma_y}\exp\left(-\frac{y^2}{2\sigma_y^2}\right) \tag{28}$$

where the first term represents the random state, and the second term is the plume state. The plume is transported at an effective velocity given by

$$U_e = \left(2\sigma_v^2 + U_m^2\right)^{1/2} \tag{29}$$

where $\mathbf{U_m}$ is the velocity obtained by taking the absolute value of the average values of the **U** and **V** components of the wind measured during the averaging period. Equation (29) is derived by assuming that the mean and turbulent velocities are the result of a vector with magnitude, $\mathbf{U_e}$, oscillating about the direction of $\mathbf{U_m}$ and that $\boldsymbol{\sigma_u = \sigma_v}$**.** The weight for the random component in Equation (28) is taken to be

$$f_r = \frac{2\sigma_v^2}{U_e^2} \tag{30}$$

This ensures that the weight for the random component goes to unity when the mean wind approaches zero.

Modeling dispersion of plumes from stacks on the shoreline needs to account for features governed by the horizontal inhomogeneity associated with the flow of air from the water to the land surface. In an area close to water, the land surface is warmer because the water heats up less rapidly than land in response to solar heating during the day. These essentially two-dimensional effects, especially those related to the temperature differences between urban and rural areas, are not treated reliably in models such as AERMOD and ISC.

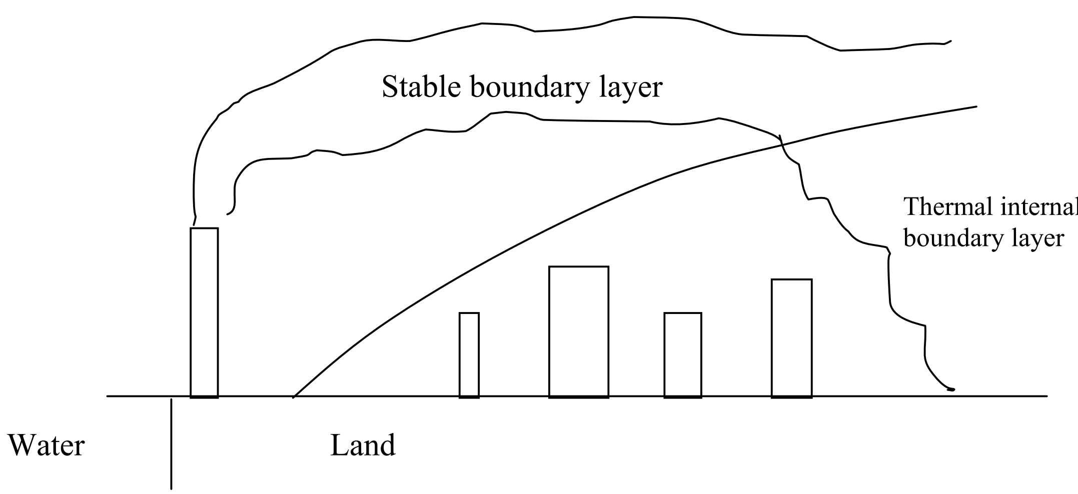

Figure 6. The growth of the urban thermal internal boundary layer (TIBL).

As the stable air from the water flows onto the warmer land, the resulting upward heat flux gives rise to an internal boundary layer that has a significant effect on the ground-level impact of elevated power plant sources. Elevated emissions, even when initially released into a stable layer, can be brought down to the ground when it intersects the growing thermal boundary layer, as shown in Figure 6. The concentration close to the point of fumigation is given by Equation (3) corresponding to the well-mixed boundary layer, where $\mathbf{z_i}$ is now the height of the boundary layer where the elevated plume intersects the internal boundary layer. It is clear that estimating the height of the internal boundary layer is important to calculating the ground-level concentration.

8 Concluding Remarks

The Gaussian model plays a critical role in the formulation of air quality models used in regulatory practice. It is really a framework that allows the incorporation of several processes that affect ground-level concentrations. We have demonstrated how it can accommodate building effects, terrain effects, and dispersion in shoreline and urban areas.

The Gaussian framework can be readily used to interpret data from field studies, and thus can be improved empirically to provide better descriptions of dispersion. These features, coupled with its computational simplicity, explain its popularity in applications that require realism as well as transparency. Although the model has shortcomings, it should not be discarded in favor of more complicated approaches unless there is a compelling reason to do so.

Acknowledgements

We would like to thank Dr. Jeetendra K. Upadhyay for his comments on this document, and Mr. Russell Lee for the support on the plume rise, building downwash, and terrain treatment.

References

Barad, M. L., 1958: Project Prairie Grass. A Field Program in Diffusion. Vol. 1 Geophysics Research paper No. 59, Air Force Cambridge Research Center, Bedford, MA.

Bowers, J.F., J.R. Bjorklund and C.S. Cheney, 1979: *Industrial Source Complex (ISC) Dispersion Model User's Guide*. Volume II, EPA-450/4-79-031, U.S. Environmental Protection Agency, Research Triangle Park, NC 27711.

Burt, E.W., 1977: *Valley Model User's Guide.* Publication EPA-450/2-77-018, U.S. Environmental Protection Agency, Office of Air Quality Planning and Standards, Research Triangle Park, NC 27711.

Cimorelli, A.J., S.G. Perry, A. Venkatram, J.C. Weil, R.J. Paine, R.B. Wilson, R.F. Lee, W.D. Peters, R.W. Brode, J.O. Paumier, 2002: *AERMOD: Description of Model Formulation (Version 02222)*, EPA-454/R-02-002d. U.S. Environmental Protection Agency, Research Triangle Park, NC 27711. Available from website http://www.epa.gov/scram001 as of January 2003.

Csanady, G. T., 1973: *Turbulent Diffusion in the Environment.* Reidel, Dordrecht, p 248.

ERT, 1987. User's Guide to the Rough Terrain Diffusion Model (RTDM), Rev. 3.20. ERT Document No. P–D535–585. Environmental Research and Technology, Inc. (now ENSR, Inc.), Concord, MA. (NTIS No. PB 88–171467).

Hanna, S.R., G.A. Briggs and R.P. Hosker, Jr., 1982: *Handbook on Atmospheric Dispersion.* Technical Information Center, U.S. Department of Energy. DOE/TIC-11223.

Lavery, T. F. *et al.*, 1982: *EPA Complex Terrain Model Development: First Milestone Report-1981* EPA-600/3-82-036, Research Triangle Park, NC p 304.

McElroy, J. L., and F. Pooler, 1968: St. Louis Dispersion Study, Volume II - Analysis. Arlington, Virginia, US Dep. HEW.

Pasquill, F. 1961: The estimation of the dispersion of wind-borne material. Meteor. Mag. 90, 33-49.

Perry, S. G., 1992: CTDMPLUS: A dispersion model for sources in complex topography. Part I: Technical formulations. *J. Appl. Meteor*. **31,** 633-645.

Schulman, L.L., and J.S. Scire, 1980: Modeling Plume Rise from Low-level Buoyant Line and Point Sources. *Proceedings, Second Joint Conference on Applications of Air Pollution Meteorology*, 24-28 March, New Orleans, LA. pp. 133-139.

Schulman, L.L., D.G. Strimaitis and J.S. Scire, 2000: Development and evaluation of the PRIME plume rise and building downwash model. *Journal of the Air & Waste Management Association*, 50:378-390.

Sheppard, P. A., 1956: Airflow over mountains. *Quart.J.Roy.Meteor.Soc.,* 82, 528-529.

Snyder, W. H., R. S. Thompson, R. E. Eskridge, R. E. Lawson, I. P. Castro, J. T. Lee, J. C. R. Hunt, and Y. Ogawa, 1985: The structure of the strongly stratified flow over hills: Dividing streamline concept. *J.Fluid Mech.,* 152, 249-288.

Taylor, G. I., 1921: Diffusion by continuous movements. *Proc. Lond. Math. Soc*.**2,** 196-211.

Thomson, D. J. and A. J. Manning, 2001: Along-wind dispersion in light wind conditions. *Boundary-Layer Meteorology* **98,** 341-358.

U.S. EPA, 1995a: *User's Guide for the Industrial Source Complex (ISC3) Dispersion Models: Volume 2—Description of Model Algorithms.* U.S. Environmental Protection Agency, OAQPS, EMAD, Research Triangle Park, NC. EPA-454/B-95-003b.

U.S. EPA, 1995b: User's Guide to the Building Profile Input Program. U.S. Environmental Protection Agency, Research Triangle Park, NC 27711.

US EPA, 1992: *User's Guide for the Industrial Source Complex (ISC2) Dispersion Models: Volume II—Description of Model Algorithms.* U.S. Environmental Protection Agency, OAQPS, Research Triangle Park, NC 27711. Publication No. EPA-450/4-92-008b.

Van Ulden, A. P., 1978: Simple estimates for vertical dispersion from sources near the ground. Atmos. Environ. 12, 2125-2129.

Venkatram, A. 1993: Estimates of maximum ground-level concentration in the convective boundary layer—The error in using the Gaussian distribution. *Atmos. Environ.*, **27(A),** 2187-2191.

Venkatram, A., 1992: Vertical dispersion of ground-level releases in the surface boundary layer. Atmos. Environ. 26A 947.

Venkatram, A., D. Strimaitis, and D. Dicristofaro. 1984. A semiempirical model to estimate vertical dispersion of elevated releases in the stable boundary layer. *Atmos. Environ.* **18**, 923-928.

Venkatram, A., R. W. Brode, A. J. Cimorelli, R. F. Lee, R. J. Paine, S. G. Perry, W. D. Peters, J.C. Weil, and R. B. Wilson, 2001: A complex terrain dispersion model for regulatory applications. *Atmos.Environ.,* in press.